

Journal of Engineering Science, Vol. 10, 95–105, 2014

Prediction of Minimum Fluidisation Velocity Using a CFD-PBM Coupled Model in an Industrial Gas Phase Polymerisation Reactor

Vahid Akbari and Mohd. Kamaruddin Abd. Hamid*

Process Systems Engineering Centre (PROSPECT), Faculty of Chemical Engineering,
Universiti Teknologi Malaysia, 81310 UTM Johor Bahru, Johor, Malaysia

*Corresponding author: kamaruddin@cheme.utm.my

Abstract: *The objective of this paper is to develop computational fluid dynamic (CFD)-population balance model (PBM) coupled model to predict a minimum fluidisation velocity in industrial polydisperse gas phase linear low-density polyethylene (LLDPE) polymerisation reactor. The population balance model (PBM) by direct quadrature method of moment (DQMOM) implemented in CFD framework was used to predict the minimum fluidisation velocity. The simulation results were validated by the operational data in terms of bed height and pressure drop. This CFD-PBM coupled model can be extended to investigate the flow field and particle kinetic through the reactor.*

Keywords: Computational fluid dynamic, population balance model, minimum fluidisation velocity, gas phase polymerisation reactor

1. INTRODUCTION

Minimum fluidisation velocity (U_{mf}) is an important fundamental hydrodynamic parameter that needs to be known in order to optimise the performance of process industry's fluidised beds reactor with a wide range of particle size distribution (PSD). Although much research has been undertaken on the U_{mf} , there are still problems often encountered in industrial applications which have not yet been thoroughly resolved. First, some of the results obtained are contradictory and based on the empirical equations. Second, there is variation of U_{mf} for particles with wide PSD, and third, variation of fluidisation behaviour also occurs from laboratory to industrial scale.

Several studies have been conducted to investigate the potentials and limitations of the CFD-PBM modelling to study the PSD in fluidised bed reactor (FBR). Oliveira et al.¹ investigated the U_{mf} for biomass and sand mixtures in acrylic fluidised bed with an inner diameter of 0.05 m and height 1.52 m to study the effect of average diameter. Their proposed correlation was in good agreement with experimental data. They found that biomass size and shape have an important influence on U_{mf} .

Caisedo et al.² experimentally investigated the U_{mf} in a 2D fluidised bed with different height and weight function for different PSD, with an inner diameter of 1 m. They reported that the U_{mf} depends on the bed height, column width and particle diameter. Asif and Ebrahim³ also experimented on the U_{mf} of five different binary-solid systems with a wide range of composition. They suggested that the minimum fluidisation velocity of binary mixture should be estimated from the physical properties of this mixture, such as composition, particle density and particle diameter, instead of measuring the minimum fluidisation velocity of each component.

In this paper, the proposed transient 2D CFD-PBM model is solved with a direct quadrature method of moments (DQMOM) to predict the U_{mf} . The performance of the modelling framework application is then highlighted for the industrial linear low-density polyethylene (LLDPE) polymerisation reactor.

2. GENERIC MULTIPHASIC CFD-PBM COUPLED MODEL

2.1 Problem Definition (Step 1)

The particle size distribution through the bed changes along with time. This is a crucial issue because PSD can affect the flow pattern, reactor efficiency and product quality. Therefore, successful CFD-PBM model for FBRs must be capable in predicting the observed changes in the particles characteristics.

2.2 Problem Specification (Step 2)

The simulated gas phase fluidised bed reactor in this research is the industrial scale LLDPE polymerisation reactor. The width of the square domain in simulation is equal to the diameter of actual reactor ($D = 5$ m). The reactors consist of three zones, namely, a fluidisation zone, a disengagement zone and a bulb section. The disengagement zone has a larger diameter ($1.2D$) than the fluidisation zone (D). The height of the reactor is 33.9 m. The fluidisation medium comprises a gas mixture of monomer (ethylene), co-monomer, hydrogen and inert gases.

2.3 Model Development and Solution (Step 3)

A generic CFD-PBM coupled modelling framework application for gas-phase polydisperse fluidised bed reactor was developed to couple the PSD in CFD framework. This modelling framework is a flexible platform and by changing the constitutive equation, its application can be extended to various polydisperse multiphasic FBRs. As shown in Figure 1, the generic model consists

of four main steps including problem definition, problem specification, model structure/solution and model applications.

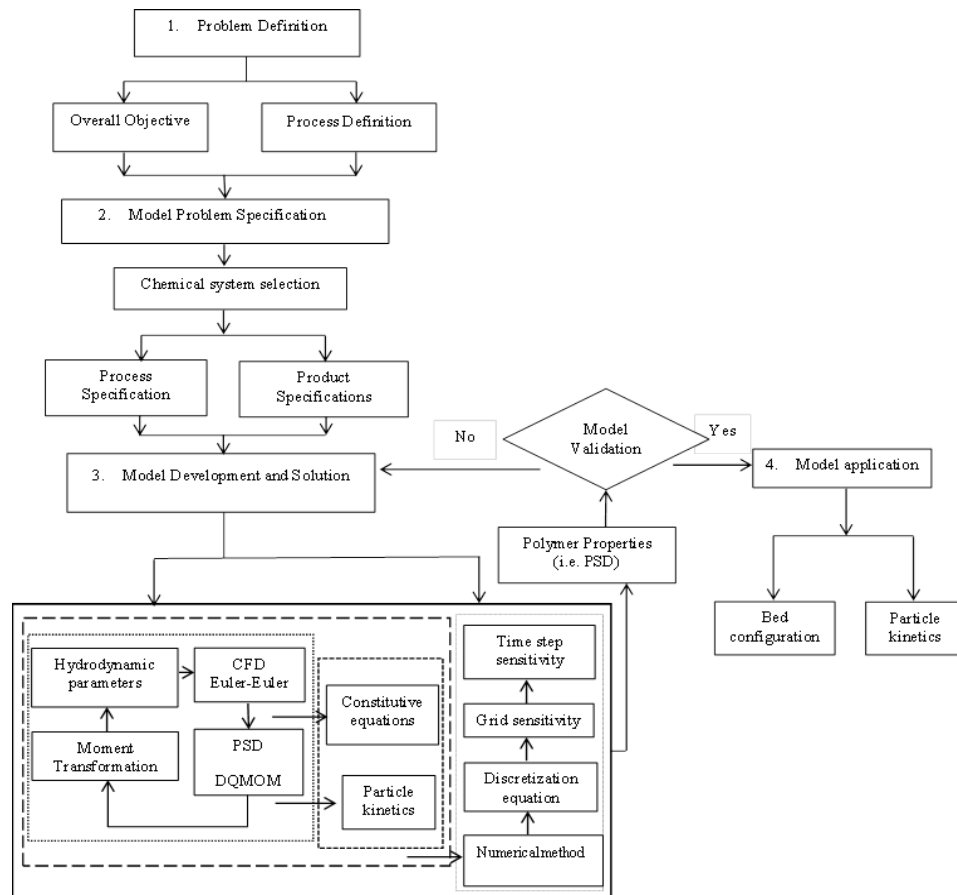


Figure 1: Generic CFD-PBM modelling algorithm for gas-solid poly-dispersed FBRs.

In order to investigate the potentials and limitations of the CFD modelling, the CFD-PBM with the Eulerian-Eulerian⁴ approach was used to investigate the effect of PSD on U_{mf} . The direct quadrature method of moment (DQMOM) was used to take into account the PSD, whereas the kinetic theory of granular flow (KTGF) was employed to close momentum balance equation for the solid phases. The phase coupled SIMPLE algorithm was used to couple pressure and velocity. In addition, Workbench Ansys 14 was used to generate the 2-dimension geometry and grids, and the obtained minimum node needed to simulate the CFD in FBR was 52007. A small time-step (0.01 s) and the convergence criterion of 10^{-3} with around 20 iterations per time-step were chosen

to ensure numerical stability is reached. Table 1 summarises the simulation condition to define the U_{mf} .

Table 1: Boundary condition and model parameters.

Description	Values	Description	Values
Granular viscosity	Gidaspow ⁴	Inlet boundary condition	Velocity inlet
Granular bulk viscosity	Lun et al. ⁴	Outlet boundary condition	Pressure outlet
Frictional viscosity	Schaeffer ⁴	Wall boundary condition	No slip for gas, free slip for solid phase
Restitution coefficient	0.8	Initial bed height (m)	10
Granular temperature	Algebraic ⁴	Initial solid volume fraction	0.5
Drag law	Gidaspow ⁴	Operating pressure (Bar)	24
Inlet boundary condition	Velocity inlet	Time step (s)	0.01
Outlet boundary condition	Pressure outlet	Superficial gas velocity (m s ⁻¹)	0.5
Wall boundary condition	No slip for gas, free slip for solid phase	Particle diameter (μm)	800–1100
		Particle density (kg m ⁻³)	850
		Gas density (kg m ⁻³)	20
		Gas viscosity	1.2×10^{-5}

2.3.1 The Eulerian-Eulerian CFD model

The multi-fluid continuum model assumes that different phases behave as interpenetration continuum and each solid species has been treated as a separate phase. Each particulate phase is characterised by the unique diameter, density and other features. A two-dimensional fluidised bed has been modelled based on an unsteady state. The continuity and momentum equations for q = gas and solid phases are:

$$\frac{\partial}{\partial t} (\varepsilon_q \rho_q) + \nabla \cdot (\varepsilon_q \rho_q \vec{v}_q) = 0 \quad (1)$$

$$\frac{\partial}{\partial t} (\alpha_g \rho_g \vec{v}_g) + \nabla \cdot (\alpha_g \rho_g \vec{v}_g \vec{v}_g) = -\alpha_g \nabla P_g + \nabla \cdot \bar{\tau}_g + \alpha_g \rho_g \vec{g} + \sum_{p=1}^n (\beta_{gs} (\vec{v}_s - \vec{v}_g)) \quad (2)$$

$$\frac{\partial}{\partial t} (\alpha_s \rho_s \vec{v}_s) + \nabla \cdot (\alpha_s \rho_s \vec{v}_s \vec{v}_s) = -\alpha_s \nabla P_s + \nabla \cdot \bar{\bar{\tau}}_s + \alpha_s \rho_s \vec{g} + \sum_{p=1}^n (\beta_{gs} (\vec{v}_g - \vec{v}_s)) \quad (3)$$

where $\bar{\bar{\tau}}_q$ is the q^{th} Phase (solid and gas) stress-strain tensor, $\beta_{gs} (\vec{v}_g - \vec{v}_s)$ is an interaction between phases and P is the pressure shared by all phases. β_{gs} is the momentum exchange coefficient between phases, $\beta_{gs} = \beta_{sg}$ and \vec{g} is the gravity vector.

$$\bar{\bar{\tau}}_q = \varepsilon_q \mu_q (\nabla \vec{v}_q + \nabla \vec{v}_q^T) + \varepsilon_q \left(\lambda_q - \frac{2}{3} \mu_q \right) \nabla \cdot \vec{v}_q \bar{\bar{I}} \quad (4)$$

μ_q and λ_q are the shear and bulk viscosity of phase q . The Eulerian-Eulerian two-fluid model requires closure equations to describe the rheology of the solid phase. Due to collisions between particles in dense gas-solid systems, the concepts from gas kinetic theory can be employed to describe the motion of particles. Several drag models are considered for the gas-solid interphase exchange coefficient β_{gs} . In this paper, the Gidaspow drag model⁴ has been utilised. The Gidaspow model is a combination of Wen and Yu model and Ergun equation.⁴ This model is recommended for dense fluidised beds.

2.3.2 The population balance model and DQMOM

A 2D CFD-PBM coupled model is based on the Eulerian-Eulerian model that incorporated the kinetic theory of granular flow (KTGF) and the PBM has been implemented to describe the gas-solid multiphase flow in the fluidised bed polymerisation reactor. In addition, The DQMOM was used to solve the population balance equation (PBE) and implement the combination of the CFD model and PBE, which represent the fundamental knowledge of the gas-solid flow pattern in the polymerisation reactor where the size is changing.

In the DQMOM each node (different solid phase) represents the solid phase properties, so in the Eulerian-Eulerian multi-fluid model each solid phase has its own momentum balance. This is in contrast to the QMOM where the moments are tracked with an average solid velocity. Thus, the DQMOM offers a promising capability in describing PSD undergoing particle kinetics in the context of CFD-PBM gas-solid modelling. This method has been described comprehensively elsewhere^{5,6} and here, only a brief review of the equations is provided. A polydisperse solid-phase can be modelled by the following multivariate distribution function.⁷

$$\frac{\partial n(L, u_s; x, t)}{\partial t} + \nabla \cdot [u_s n(L, u_s; x, t)] + \nabla_{u_s} \cdot [F n(L, u_s; x, t)] = S(L, u_s; x, t) \quad (5)$$

where \mathbf{x} is the spatial coordinate and t is time. In Equation 5, $S(L, u_s; x, t)$ is a source term that represents discontinuous changes in property space due to kinetic particles, whereas F is the force to accelerate each solid phase. The mean force, F , conditioned over the particle diameter L and defined as $\langle F | L = L_k \rangle$ acts to accelerate the particles of solid phase k . $\langle u_s | L \rangle$ is the mean velocity conditioned on the particles of diameter L . By definition, $\langle u_s | L = L_{sk} \rangle$ equals u_{sk} for the k^{th} solid phase particles. The DQMOM approach also uses number density function $n(L; x, t)$ and quadrature approximation by a summation of N Dirac delta functions:

$$n(L, u_s; x, t) = \sum_{\alpha=1}^N \omega_{\alpha}(x, t) \delta[L - L_{\alpha}(x, t)] \delta[u_s - u_{s\alpha}(x, t)] \quad (6)$$

where ω_{α} is the weight of the delta function centred on the characteristic length, L_{α} . By inserting Equation 6 into Equation 5, and applying a moment transformation, the population balance in terms of the presumed finite mode PSD can be shown as in Equation 7.

$$\sum_{\alpha=1}^N \delta(L - L_{\alpha}) \left[\frac{\partial \omega_{\alpha}}{\partial t} + \nabla \cdot (\omega_{\alpha} u_{s\alpha}) \right] - \sum_{\alpha=1}^N \delta(L - L_{\alpha}) \left[\omega_{\alpha} \left(\frac{\partial L_{\alpha}}{\partial t} + u_{s\alpha} \cdot \nabla L_{\alpha} \right) \right] = S(L, T) \quad (7)$$

The weights and abscissas can be correlated with the solid volume fraction and the effective particle diameter (length) for each solid phase. The transport equations for each weights and abscissas undergoing growth, aggregation and breakage rate can be written as follows⁷:

$$\frac{\partial \varepsilon_i \rho_s}{\partial t} + \nabla \cdot (\bar{u}_{si} \varepsilon_i \rho_s) = 3k_v \rho_s L_i^2 (b_i + w_i G_i) - 2k_v \rho_s L_i^3 a_i \quad (8a)$$

$$\frac{\partial \varepsilon_i L_i \rho_s}{\partial t} + \nabla \cdot (\bar{u}_{si} \varepsilon_i L_i \rho_s) = 4k_v \rho_s L_i^3 (b_i + w_i G_i) - 3k_v \rho_s L_i^4 a_i \quad (8b)$$

where ε_i and $\varepsilon_i L_i$ are the volume fraction and the effective particle length, respectively. w_i is the number of particles per unit volume and G_i is the growth rate at Quadrature point, while a_i and b_i can be computed through a linear system resulting from the moment transformation of particle number density transport equation using N Quadrature points.⁷ k_v is a volumetric shape factor (equal to $\pi/6$ for spherical particles). Equation 8a represents the conservation equation for the volume fraction of the k^{th} solid phase in the presence of growth rate, while Equation 8b is a conservation equation for the effective particle diameter. Further details on derivation and solving these equations can be found elsewhere.⁵⁻⁷

2.3.3 The CFD-PBM coupled model

In step 3 of the generic algorithm for coupling CFD-PBM modelling, the PBM model needs to be coupled with the multi-fluid CFD model. The algorithm for such coupling is as follows:

Step 1: Solve the multi-fluid Eulerian-Eulerian equations (Equations 1 to 4) at every grid point. From the CFD model, we obtain the hydrodynamic parameters such as solid volume fraction, particle diameter and particle velocity.

Step 2: Solve the PBM equations (8a and 8b) for the PSD using solid volume fraction and solid velocity of step 1, and particle growth rate for each solid phase.

Step 3: Using moment transformation to define sauter mean diameter of solid phases and update the hydrodynamic parameters, and repeat steps 1–3 for next iteration.

2.3.4 Model validation

The CFD-PBM coupled model has been validated by comparing the simulated results and the industrial data obtained by an industrial LLDPE gas-phase polymerisation reactor. To validate this work, the distribution of the particle sizes inside the reactor was considered to be similar to the product particle size distribution.

Figure 2 and Figure 3 show the transient behaviour of pressure drop and bed height and their comparison with the industrial data. As can be seen in Figure 2 and Figure 3, the whole simulation process can be identified as two stages: a start-up stage and a quasi-steady fluidisation stage. The steady state bed height in the gas-solid flow was reached after 73 s, while the pressure drop usually oscillates inside its operational range due to the fluidisation

characteristics. The predicted pressure drop and the bed height profile along the time showed very good agreement with the industrial data, where 1.25% and 0.75% error were observed in predicting the pressure drop and bed height respectively (see Figure 2, Figure 3 and Table 2).

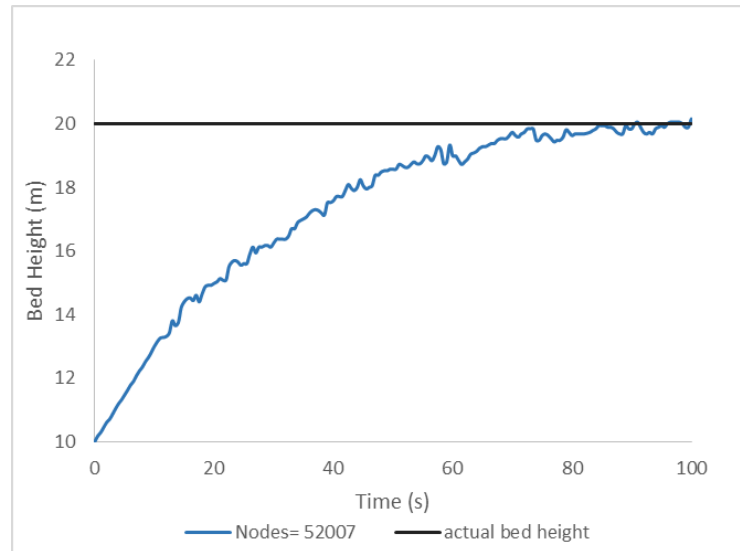


Figure 2: Comparison of the CFD predicted bed height data with industrial data.

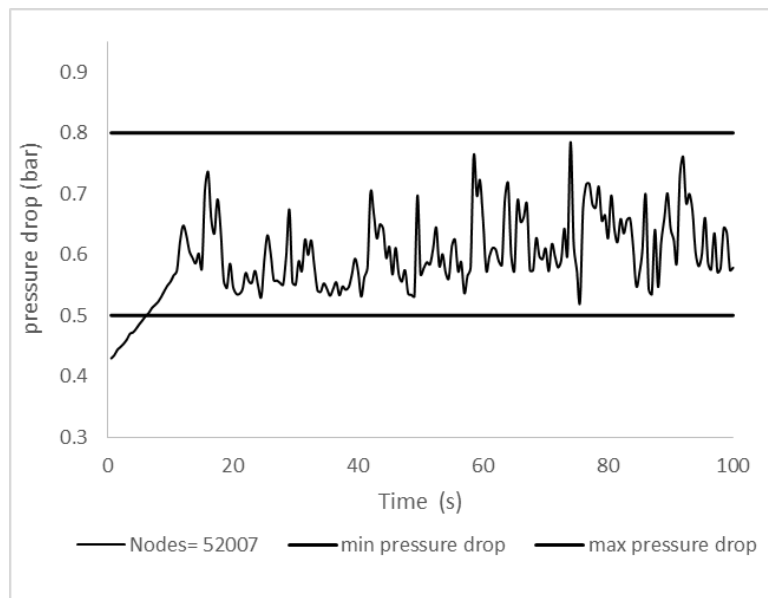


Figure 3: Variation of bed pressure drop superficial gas velocity.

Table 2: Comparison between industrial data and CFD simulated results.

Parameter	Simulated result	Industrial data	% Bed height error	% Pressure drop error
Final bed height	20.15	20	0.75	–
Average pressure drop	0.578	0.588	–	1.24

2.4 Model Application (Step 4)

2.4.1 Pressure drop and minimum fluidisation velocity

Figure 4 shows the variation of pressure drop for various superficial gas velocities to define U_{mf} in the simulated reactor. With increasing gas velocity, the bed pressure drop increases along the fixed bed ($U_{mf,f}$), where all small and large particles are still stagnant. After ($U_{mf,f}$) the pressure drop deviates from the curve representing the performance of the fixed bed reactor. This is due to the segregation of small particles and partial de-fluidisation of solids at the bottom of the bed. This period reaches a peak at $U_{mf,j}$. By further increasing the gas velocity, the pressure drop will be decreased slightly due to small particles which tend to fill the coarse inter particle voids although the coarse particles remain unchanged. At the point shown by (U_{ff}), it is seen that the bed is steadily fluidised and effective bed mixing overshadows the de-fluidisation at the bottom of the bed. Also, at (U_{ff}), the total pressure drop equals the weight of the whole bed.

The U_{mf} condition of FBRs is defined at point A where the rising pressure drop line representing the state of fixed bed meets the constant pressure drop line representing the status of fluidisation state along with variation of the gas velocity. It can be assumed that both small and large particles are not fully fluidised at point A. This is an intermediate state between the minimum fluidisation velocity of small particles and the minimum velocity at which the bed is completely fluidised.

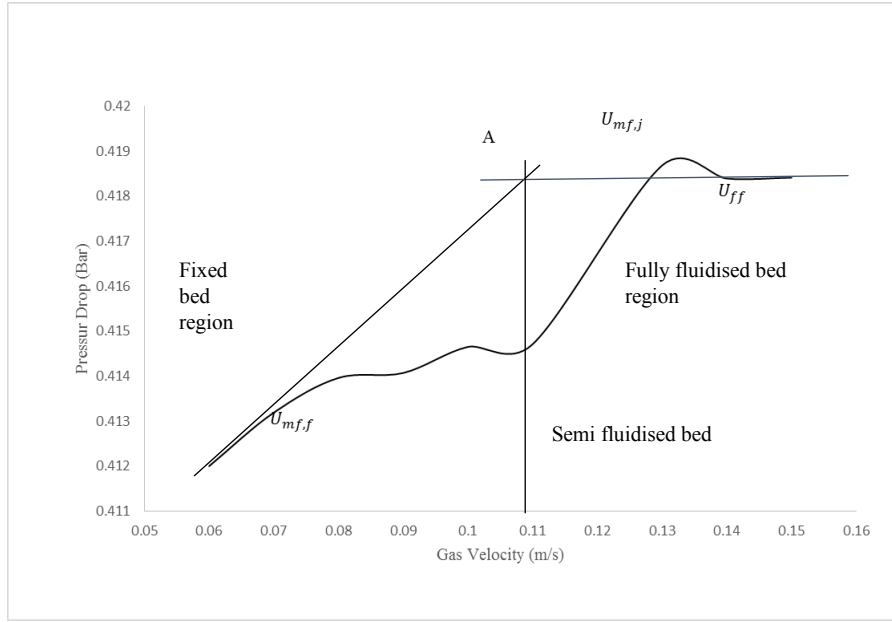


Figure 4: Determination of U_{mf} from the pressure drop with gas velocity.

In this study, the minimum fluidisation condition of polydisperse is defined as the point U_{ff} . For the simulated reactor, U_{mf} is equal to 0.14 m s^{-1} . Here, the computational values of U_{mf} based on Equation 9⁴ are used to verify the CFD prediction. According to Equation 9, U_{mf} for small and large particles can be obtained as 0.1 and $0.15 \text{ (m s}^{-1}\text{)}$ respectively. The comparison of these data proves that the CFD predictions are in good agreement with the results of Equation 9. The difference between the predicted values by two models in the present study is lower than 6.6%.

$$U_{mf} = \frac{\mu}{d_p \rho_g} \left\{ \left[33.7^2 + 0.408 \frac{d_p^3 \rho_g (\rho_p - \rho_g) g}{\mu^2} \right]^{1/2} - 33.7 \right\} \quad (9)$$

3. CONCLUSION

In this study, a generic CFD-PMB framework was developed to investigate the effect of the method for estimating the U_{mf} of PSD in polymerisation gas-solid fluidised bed reactor. Results of the model were first compared to the real industrial LLDPE FBR. The U_{mf} value for PSD can be calculated by Wen and Yu⁴ with fairly good agreement. This generic CFD-PBM

prediction will provide useful information for the design of FBR systems with potential application for dryers, polymerisation and solid catalysed chemical reaction.

4. ACKNOWLEDGEMENT

Financial support from Universiti Teknologi Malaysia under grant number RJ130000.7844.4L036 is gratefully acknowledged.

5. REFERENCES

1. Oliveira, T., Cardoso, C. & Ataíde, C. (2013). Bubbling fluidization of biomass and sand binary mixtures: Minimum fluidization velocity and particle segregation. *Chem. Eng. Process.: Process Intens.*, 72, 113–121.
2. Ramos Caicedo, G. et al. (2002). Minimum fluidization velocities for gas–solid 2D beds. *Chem. Eng. Process.: Process Intens.*, 41(9), 761–764.
3. Asif, M. & Ibrahim, A. A. (2002). Minimum fluidization velocity and defluidization behavior of binary-solid liquid-fluidized beds. *Powder Technol.*, 126(3), 241–254.
4. Chen, X.-Z. et al. (2011). A fundamental CFD study of the gas–solid flow field in fluidized bed polymerization reactors. *Powder Technol.*, 205(1), 276–288.
5. Mazzei, L., Marchisio, D. L. & Lettieri, P. (2009). Direct quadrature method of moments for the mixing of inert polydisperse fluidized powders and the role of numerical diffusion. *Indust. Eng. Chem. Res.*, 49(11), 5141–5152.
6. Marchisio, D. L. & Fox, R. O. (2005). Solution of population balance equations using the direct quadrature method of moments. *J. Aerosol Sci.*, 36(1), 43–73.
7. Fan, R., Marchisio, D. L. & Fox, R. O. (2004). Application of the direct quadrature method of moments to polydisperse gas–solid fluidized beds. *Powder Technol.*, 139(1), 7–20.